Comparison and analysis of turbine wake interaction

Mallory Elise Flowers
Summer Undergraduate Laboratory Internship,
Ames Laboratory, Department of Energy
Mentors: Dr. Eugene S. Takle and Daniel A. Rajewski

ABSTRACT

Air moving through a series of turbines generates wake conditions that interact to change local wind patterns. Correspondingly, the power output at downwind turbines can change. An improved understanding of how these wakes impact power generated throughout a wind farm is vital to achieving the DOE goal of reducing the levelized wind energy cost. The degree of power loss due to wake interference has high variability, but previous research has not identified contributing factors. This study's objective is to better understand how single and multiple turbine wakes impact the power output of a wind farm. Statistical and numerical analysis techniques were used to analyze atmospheric conditions that might influence wakes, such as wind speed and direction, temperature, and the concurrent surface layer stability, turbulence, net radiation, and air pressure in the agricultural field surrounding the wind farm from which data was collected. Observations show that wind speed drops significantly after the first turbine, and then gradually recovers to about 75% of its original speed while passing through the next turbines within 1.5 km downwind. Power generated at downwind turbines follows a similar pattern: a second turbine located less than 4 rotor diameters downwind of the lead generates just over 40% of the power generated at the lead turbine, and recovers down the line. Atmospheric conditions greatly influence the recovery rate of wind speed and power generated. Wakes in this study appeared to dissipate more quickly than in other offshore studies.

I. INTRODUCTION

As wind flows through lines of turbines, the power harvested at each successive turbine changes, largely due to turbines interacting via the wake generated by the rotating blades.

Changes in wind throughout a line of turbines or wind farm can have significant impacts on the power generated by these turbines. When wind blows straight down a line of turbines, the lead turbine often produces much more power than turbines in its wake. These drops in power production correlate roughly to the wind speed deficit in the turbine wakes. However, there is still much to be learned about how this interaction occurs.

Until recently, wake research was highly limited, and even now much of the research is focused on offshore wind applications rather than land-based wind farms. Throughout various studies for turbines offshore in Northern Europe (Barthelmie, 2005, 2007, 2008, 2009, 2010), one theme is clear: though we have many tools by which to observe, compare, and predict turbine interactions, many uncertainties remain. The variables determining how turbine wakes interact are complex and interconnected, limiting our ability to predict them. It can also be difficult and expensive to collect the types of data required in order to validate and improve extant models. In addition, gathering turbine data sufficient enough to validate these models under the diurnal and seasonal weather conditions that wind farms experience is often expensive and time-intensive. It is unclear as to whether the analysis from offshore turbines is valid for land-based operations.

Hegberg (2004) used wind tunnel observations to evaluate existing models predicting turbine interaction. He concludes that, while existing models predict a return to equilibrium conditions 5 turbines (or turbine rows) downstream from the lead turbine, some data show that 10 turbines are required, indicating that existing models tend to over-predict power output at a wind farm. Additional data from land-based farms are needed to assess the validity of existing models and to document the need for new models for on-shore turbine wake interactions.

Being able to accurately and dependably predict the way that these wakes impact power output on a wind farm is crucial to optimizing wind farm design and operation. Wake models have been previously generated, but are mostly intended for offshore applications, and have high levels of uncertainty and variation in the analysis. This paper will explore the impacts of single and multiple turbine wakes on downwind turbines. Numerical analysis techniques will be used to seek patterns in the data collected from a small set of turbine lines, ranging from two to six turbines in length.

II. EXPERIMENTAL METHODS

The data analyzed comes from the Crop/Wind-energy EXperiment (CWEX) 2010 and 2011 data sets from a central Iowa utility. The CWEX archive includes field measurements within a wind farm to understand how wind energy, meteorology, and crop agriculture interact. Nacelle data come from 1.5 MW turbines with a hub height of 80 m, with 3 blades and a rotor diameter of 77 m. Rated for 12 m/s, these turbines cut-in at wind speeds of 3 m/s and cut-out at 25 m/s.

Figure 1 shows the turbines observed, comprised of two lines, both oriented along the East-West direction. The A-line is composed of 5 turbines and sits North of the B-line, composed of 8 turbines. With the exception of B7 and B8, both sets of turbines were equally spaced along their respective lines, 282 m (roughly 3.8 rotor diameters) apart. Turbine B7 sits 550 m to the Northeast of B6 (300 m East and 460 m North). Turbine B8 is located in the same direction as B7 from B6, 282 m beyond B7.

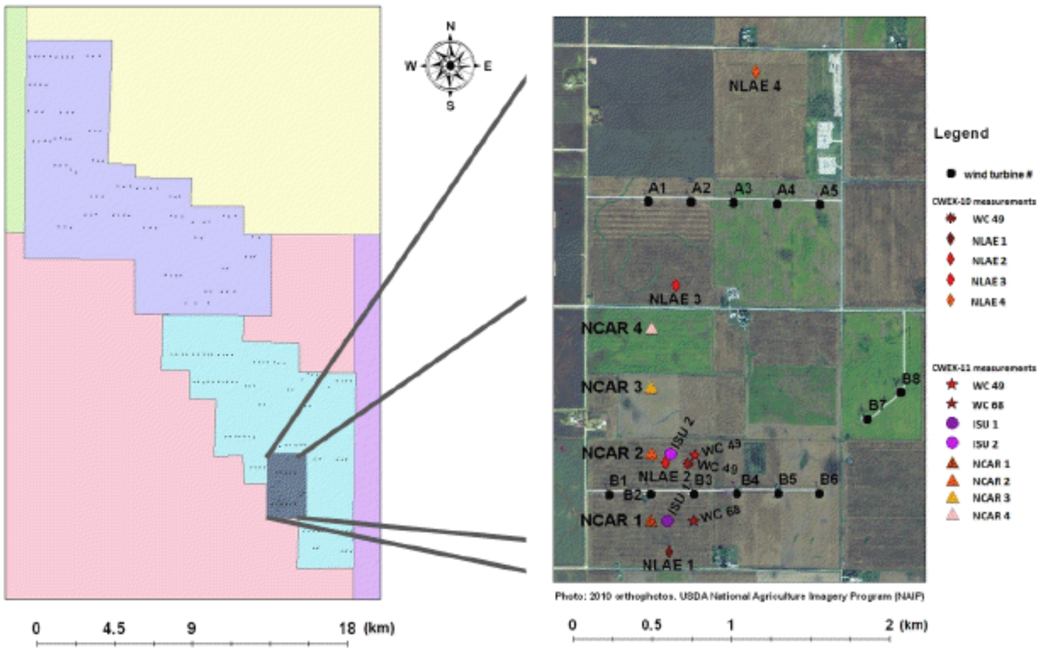

Figure 1: Overlay of the wind farm boundaries with an expanded view of the measurement locations for CWEX-10 and CWEX-11.

The data consist of 10-min averages of higher frequency nacelle-based wind speed, direction (yaw angle), temperature, and power generated for each turbine. Wind speed is measured behind the blades of turbines as they face the wind, usually coming from the South. Thus, data does not represent free stream airflow, but gives a consistent estimate of the speed at all times.

Surface flux stations in the surrounding agricultural fields provided data on heat, moisture, and CO_2 flux; mean and turbulent wind components; leaf wetness; relative humidity; and incoming and outgoing radiation levels (short and long wave). Analysis will focus on data related to the wind speed and direction, power generated, and concurrent surface-level temperature, radiation, and atmospheric stability.

Investigation of the power output among the turbines included its variation seasonally and diurnally, as well as its dependence on wind direction, stability, pressure, density, humidity, and temperature. Both the wind speed and power generated at each nacelle vary most when the wind direction aligns with the line of turbines (due East or West). The normalized (ratio of value at a downwind turbine to the lead turbine) power and wind speed were analyzed to evaluate wake interactions. For this, the lead turbine always has a normalized ratio of 1, while the ratio for the following turbines usually have a value less than one.

Wind directions defined as easterly were between 75˚ and 105˚ (90˚±15˚), and west winds were defined as from 255˚ to 285˚ (270˚±15˚). All complete sets of data (numbering about 282 for the east data, and 195 for the west data) were included in initial analysis.

Because the trends were highly similar for both lines, the separation of the A-line and B-line for this proved unnecessary for some portions of the study (though only the B-line was used in the analysis of the sixth turbine in line). Creating subsets of these data by for diurnal time periods, wind direction, and year allowed trends to be verified from one sample to another.

The normalized power ratio at each turbine closely reflects the normalized wind speed ratio at that turbine. Factors affecting these ratios include distance from the turbine projecting the wake, and the number of successive wakes. Changes in these ratios for each turbine were evaluated for a variety of other variables (horizontal wind speed, pressure, stability, etc.).

To help quantify these relationships, techniques from numerical linear algebra were employed to help determine the overall significance of each variable in determining the wind speed deficit. The MATLAB code used in doing so is included in the appendix to this paper.

In addition to this code, it should be noted that meteorological formulas were employed to extrapolate some data analyzed in this study. Stability at surface level, power generated by turbine, and pressure at hub height were calculated according to the following formulas, in which L_{sfc} represents surface stability, while θ_v, u_*, kg, and $w_{ts\_4.5m}$ represent potential temperature, friction velocity, mass, and vertical velocity, respectively. Additional variables, such as ρ (density), C_p (turbine power coefficient), A (swept area of rotor), $\bar{u}_{hub}$ (average velocity at the hub height), P_{hub} (pressure at hub height), P_{sfc} (pressure at surface), g (force due to gravity), z (altitude), R (ideal gas constant), T_{avg} (average temperature between surface and turbine height) were also utilized.

$$L_{sfc}=\theta_v u_*^3/(kgw_{ts\_4.5m})$$
$$Power=\tfrac{1}{2}\,\rho C_p A\bar{u}_{hub}^3$$
$$P_{hub}=P_{sfc}\times\exp(g\Delta z/RT_{avg})$$

To observe wake impacts over greater distances, it was useful to also look at instances when wind direction followed across turbine lines. By projecting a 5 degree wake out from each turbine, the impacts of turbine wakes at other distances could be observed. The unique positioning of turbines B7 and B8 permitted analysis of a variety of numbers of wakes interacting. Depending on wind direction, these two turbines may be operating under free stream conditions, or in the wake of from one to three turbines, all at different distances. For example, Fig. 2 shows projected wakes for a yaw of 248˚, in which B7 is potentially under the influence of wakes from B1, B2, B3, and B4, but not B5 or B6. Additionally, the impacts of the B-line wakes on the A-line were also investigated. The results of this analysis were compared to the previous analysis preformed.

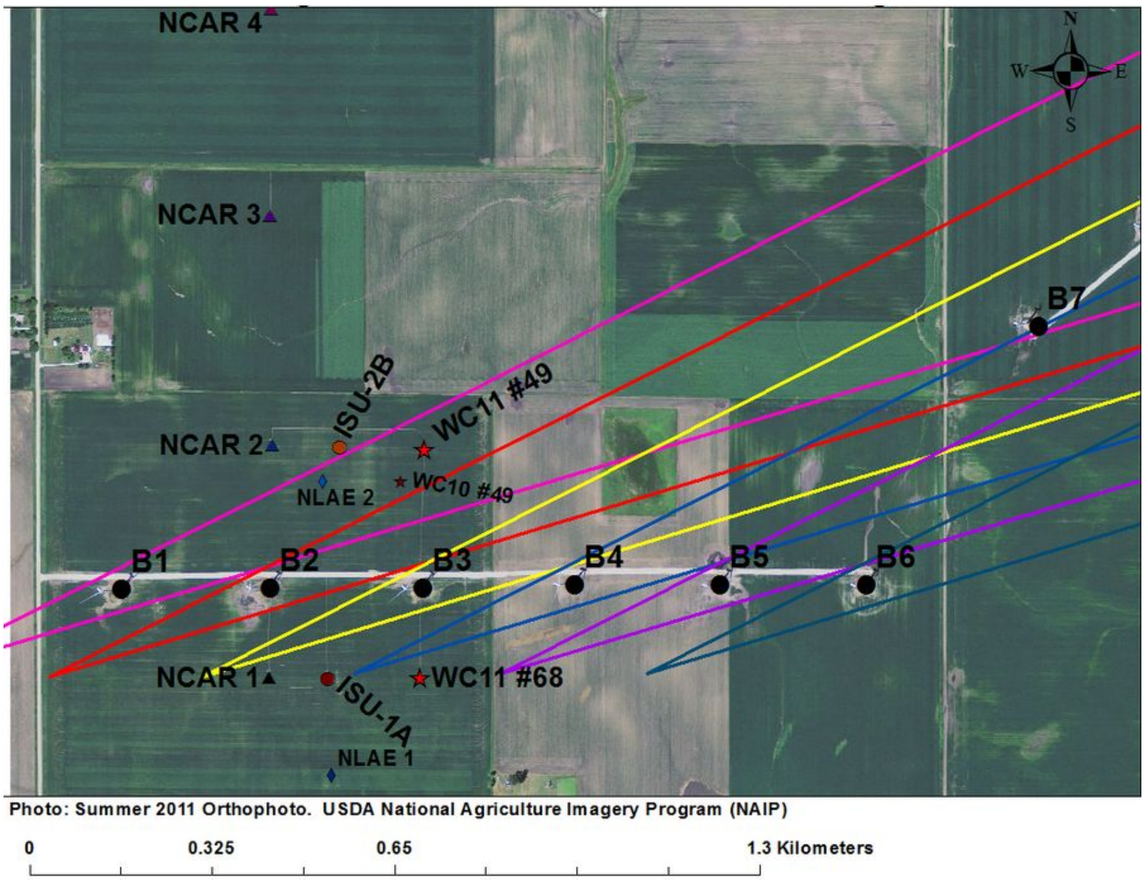

Figure 2: *Five-degree wakes projected from a Southwest direction towards B7 and B8.*

Note that the raw data used to execute these calculations is confidential. Therefore, only certain data is included in this report. Rather than report the wind speed or the power generated at the site, the normalized wind speed and power ratios are listed. This does not impede the accuracy or validity of the trends observed.

III. RESULTS

Power generated as wind moves directly down the line of turbines drops most severely after the first turbine, and then gradually increases from that point, to approximately 60-70% of its initial value at the lead turbine. Wind speed drops similarly after the first turbine, and appears to level off around 80% of its original value. This trend is clear in Fig. 3. Here, the median power ratio and wind speed ratio for each turbine (compared to the first turbine in line) is shown for both the East and West wind directions. Vertical lines at each turbine represent the range of occurrence for the middle 50% of data collected. This spread may be due to changes in atmospheric conditions.

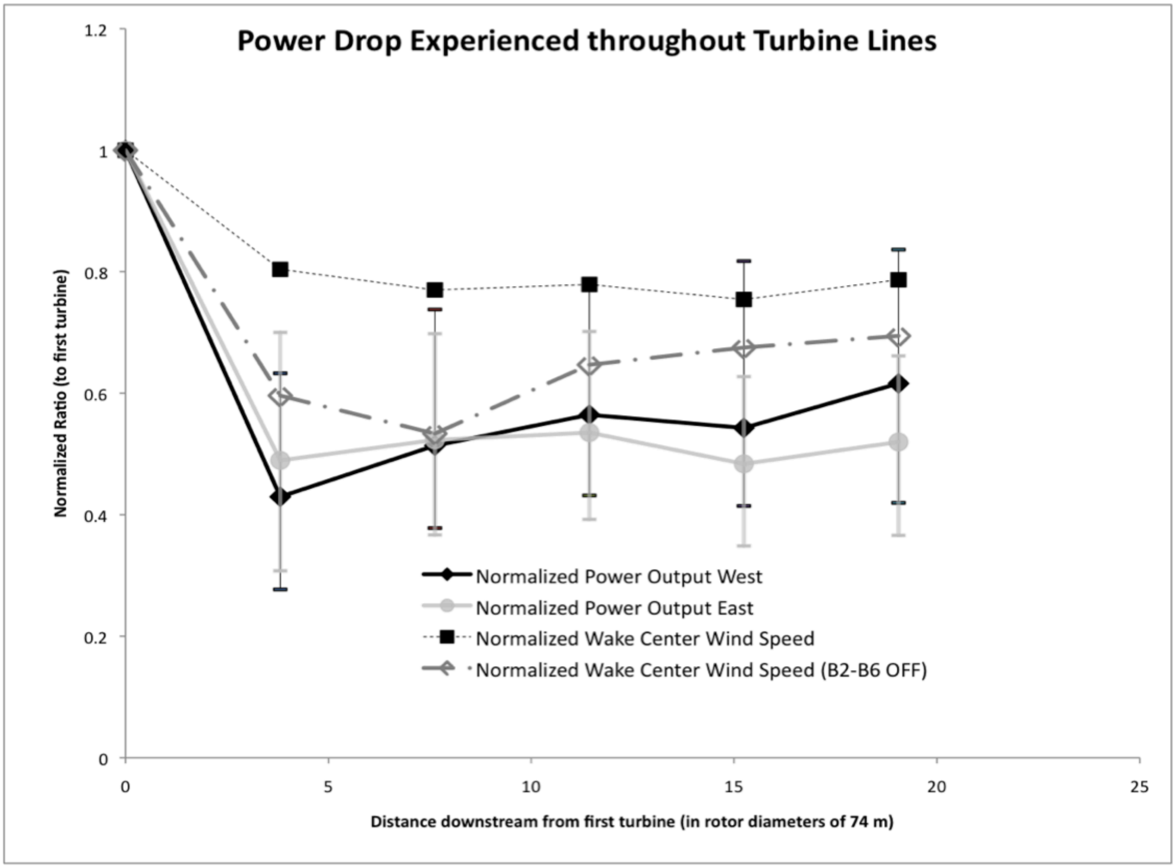

Figure 3: *Power and wind speed trends throughout the line of turbines. Data includes East and West wind events.*

To facilitate an understanding of the impact of atmospheric conditions on turbine wakes, the data collected were organized into a series of plots (Fig. 4) mapping each turbine and the relative power it generated at a certain time against one other atmospheric variable. This was done for surface level turbulence, net radiation, pressure, and stability. Additionally, hub height measurements of the wind speed, wind direction, and temperature were considered. Time of day was also considered as a method for partitioning data into comparable samples. Appendix B includes various plots that were not included in Figure 4.

The relationship between each variable and its impacts on turbine wakes were quantified. The same data sets used for Figure 4 were treated as over-determined matrices and generating the corresponding singular value decomposition matrices, then finding the least-squares solution to the set in order to approximate a linear relationship between the variables and the wake impact on wind speed. Figure 5 demonstrates the strength of these relationships as compared to the other variables analyzed. Note that the Turbine 6 results are based only on the B-line of turbines. The chart in (a) represents averages from both turbine lines in 2010 and 2011, plotted in (b). Though the numbers varied by year and turbine line, the variance was small at all turbines except the fourth downstream.

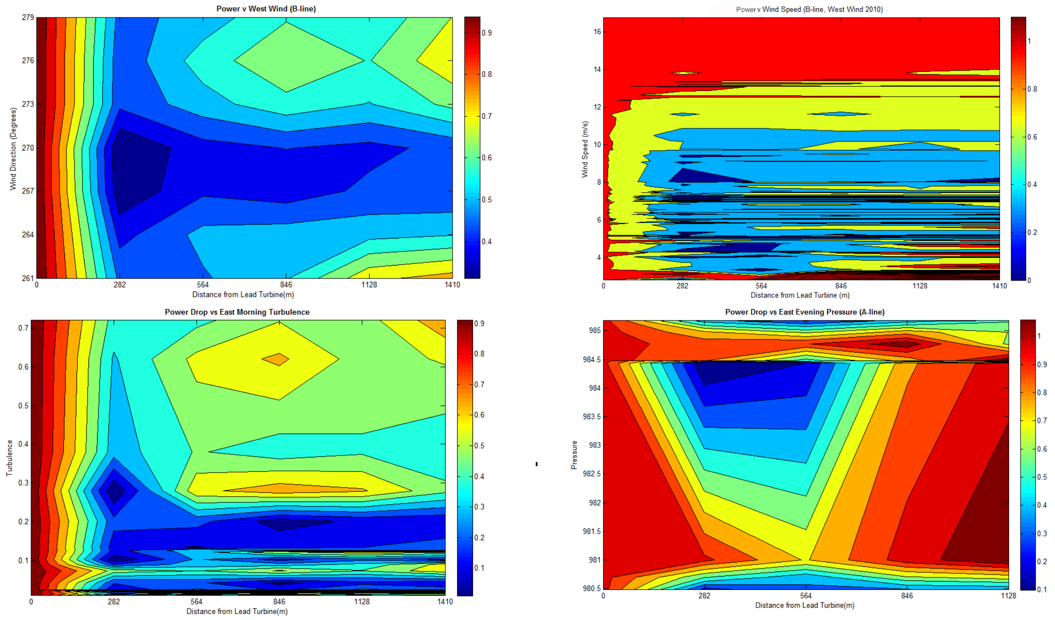

Figure 4: *Contour plots reflecting changes in power generated as a result of patterns in wind speed throughout the turbine line, with respect to various conditions. Representative samples of these plots for wind direction (upper left), wind speed (upper right), surface-level turbulence (lower left), and pressure (lower right) at the hub height are plotted here, and additional plots of this type can be found in Appendix B.*

As seen in Figure 4, maximum wake impact occurs near the initial turbine, and beyond that the wake appears to decay with distance. To better understand the relationship between distance and the strength of the turbine wake, the impacts of the main B-line of turbines (B1-B6) on turbine B7 were studied (Fig. 6). Southwest wind conditions were compared to the wind speed ratio between the nearest upwind turbine and turbine B7. The ranges of wind directions for which each turbine influenced B7 are mapped below the ratios.

(a)

	Relative Weights				
Variable	Turbine 2	Turbine 3	Turbine 4	Turbine 5	Turbine 6
Surface Temp	0.078100	-0.000625	122.16987	0.324825	0.0133
Horizontal Wind Speed	0.925250	1.000475	-151.58120	0.374730	0.7082
Wind Speed	0.000150	0.000000	1.27829	0.013275	-0.0151
Turbulence	-0.000975	0.000050	134.07620	0.385425	0.0769
Net Radiation	-0.004750	-0.000025	-75.47892	-0.252075	0.1445
Hub Pressure	0.000225	0.000000	-2.98907	-0.017325	-0.0026
Stability	0.000500	0.000000	5.02692	0.011775	0.0000

(b)

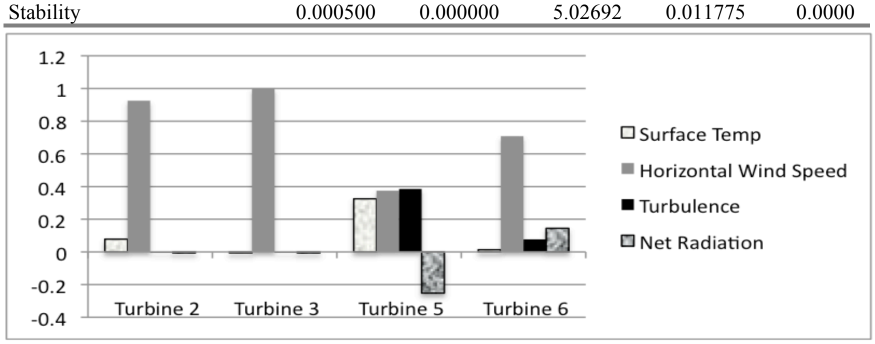

Figure 5: *Relative weights of atmospheric conditions considered in this study, found at each turbine in the line. Data in chart (a) reflect the importance of each condition in determining the impacts of turbine wakes at a wind farm. Part (b) displays some of these data that have strong linear correlations to the waked wind speed. Results from Turbine 4 appear highly unstable, and were excluded from the chart in (b).*

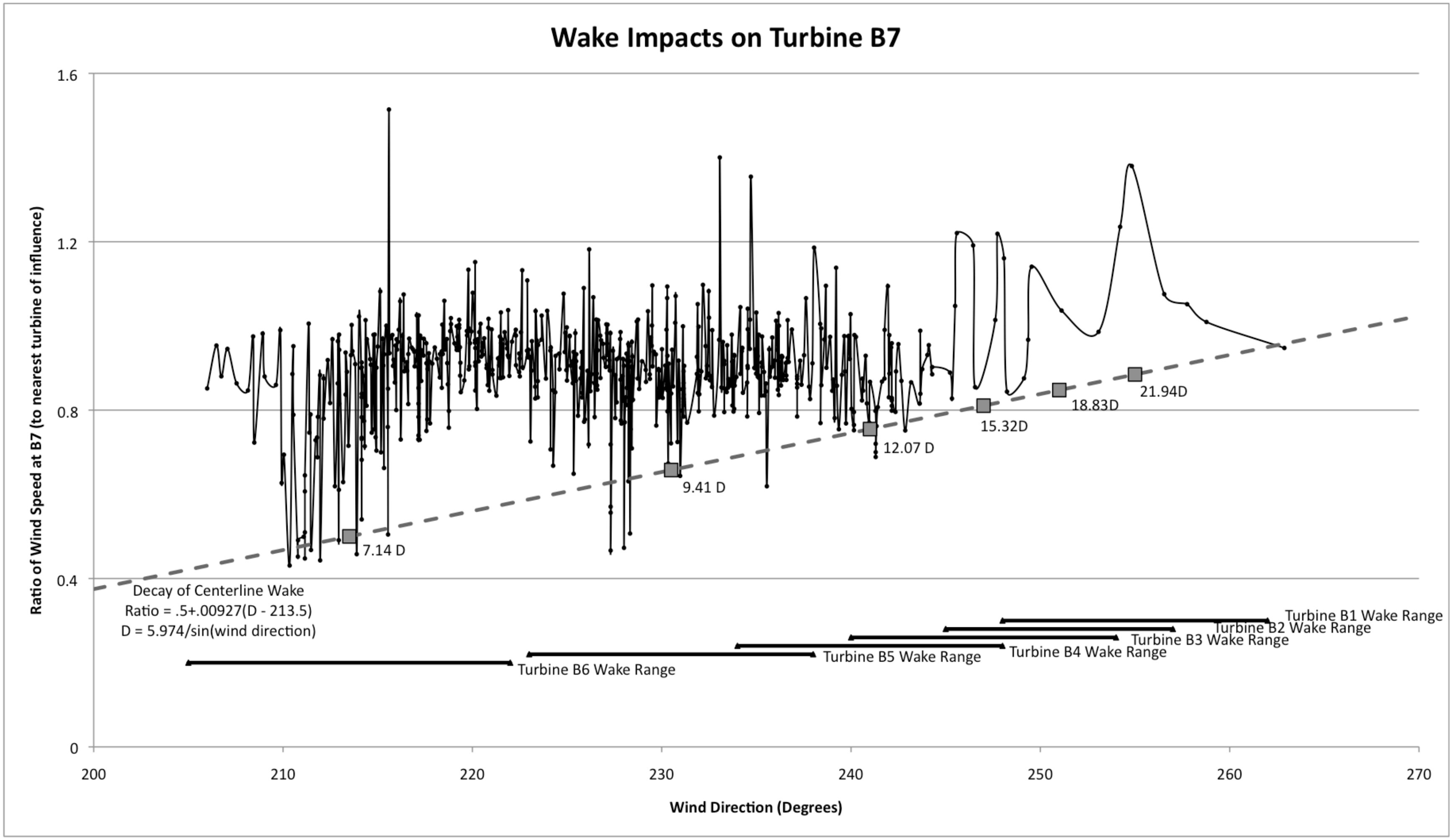

Figure 6: *Wake impacts on turbine B7 under Southwest wind conditions. The relative wind speed is plotted against the wind direction. The yaw domain of each turbines' influence is plotted below, the ratios, with the approximate wind speed ratio for the center of each domain plotted.*

At the center of each turbine's directional range of influence, the approximate wind speed ratio is plotted. Comparisons of these values to the corresponding distances they represent were used to generate Figure 7. Data at extreme angles of this plot, where not much data was available to verify results, were interpolated for consistency.

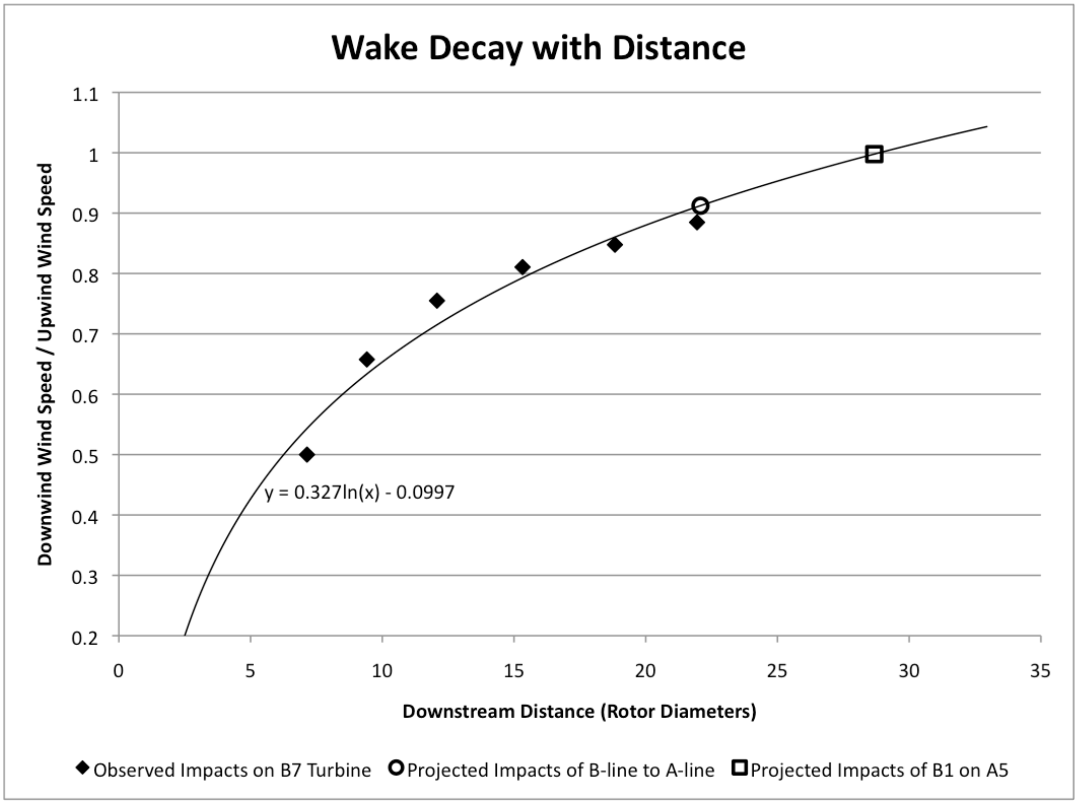

Figure 7: *Wind speed ratios from the center of each impacting wake plotted against the distance over which the wake is observed. A logarithmic trend line maps these points along with wake impact predictions for longer distances. Data collected at these distances is not disparate from this prediction.*

The logarithmic trend line plotted in Figure 7 was used to predict the wake impacts at distances even longer than those observed in Figure 6. The distance between the B and A lines (about 23 D) and the distance between B1 and A5 (about 28 D) were included as projected points on the plot shown in Figure 7. Observations of wake impacts at this distance confirmed that wakes had little impact on wind speed and power over this range, and ratios calculated reflect those projected in Figure 7.

In both the projected and observed instances, it was unclear as to whether the wakes have impact on the wind speed and power ratios at these longer-range distances. The observed ratios exceeded one in many observed instances, and no trends were observed between the atmospheric conditions analyzed and the strength of wakes at these distances.

IV. ANALYSIS AND INTERPRETATION

Though one might think the wakes compound successively down the line, and thereby repeatedly reduce the wind speed, Figure 3 demonstrates this is not the case. Rather, the greatest drop in power occurs at the second turbine in line. As the wind flows further through the system of turbines, it does not drop off continually, but seems to gradually "recover" in speed as more turbines are passed.

The results agree with the study of an offshore wind farm by Barthelmie and Jensen (2010), in that the initial drop is strongest, and although secondary drops may occur, power and wind speed both recover somewhat with distance down the line of turbines. In both cases, it is clear that the power deficit ("normalized ratio") at each turbine closely reflects the wind speed deficit at that turbine. Therefore it is vital that we understand wake impacts on wind speed, in order to dependably predict power output. In contrast to the Barthelmie and Jensen results from larger, offshore turbines, the decline in power and wind speed at the Story I & II turbines is much lower, and recovers with less distance.

Results shown in Figure 4 are very consistent for all times and turbine lines for some variables, but do not return consistent results for others. From these graphs, it is clear that wakes have the greatest negative impact on power generation as the air flows directly down the line of turbines. At wind speeds above the speed for which the turbine is rated, wake effects appear to be minimized. Variations in the wake effects at speeds less than this may be due to changes in the turbine power coefficient, as farms feather the blades to permit more air to pass through the turbine at higher speeds. For other conditions, trends were more difficult to visually determine. This can be due to scatter in the data over the narrow range of conditions experienced, "jamming" the plot with many discontinuous points. For example, the plots included in Figure 4 seem to indicate that wake impacts are minimized under turbulent and/or high pressure conditions, but other plots of similar data from other timeframes or turbine lines were less clear. Therefore, numerical techniques were of great useful in determining relationships for these and other conditions.

The strength of the wake correlates strongly to horizontal wind speed (Fig. 5). In the near-wake region close to the lead turbine, horizontal wind speed is nearly an exclusive indicator. Farther downstream however, this relationship weakens, and other atmospheric conditions become increasingly significant. Turbulence, temperature, and net radiation appear to have strong influence over the wake pattern at greater distances.

It is uncertain which of these have the strongest influence at various distances, as these conditions are not completely independent. This method for comparison enables multi-variable analysis, but is limited to linear relationships. It is possible that greater specificity could be achieved by investigating potential non-linear relationships between these conditions and the wake effects. These limitations could also explain the inconsistent results found at the fourth turbine, where this method of analysis does not appear to be effective. The distance to turbine 4 corresponds roughly to the boundary between the near- and far-wake patterns, which according to other analysis (Duckworth and Barthelmie, 2008), could be an alternative explanation for inconsistent results.

In Figure 6, it can be noted that wake effects increase towards the centerline of each turbine wake. The plot dips in three distinct locations, each of which correspond to the angles at which the B6, B5, and B4 turbine wakes point directly into the B7 turbine. This indicates that the wake impacts on wind speed are strongest in the centerline of the wake. It can also be noted that the change in wind speed is most extreme at close range. Turbine B6, about 7 D upwind from B7, has the strongest impact on turbine B7. Turbines B5 and B4 have subsequently weaker effects on wind speed as the distance between the turbines increases.

The wake interactions between turbines B1-3 and B7 are less clear. The yaws in which these turbines impact B7 overlap a good deal, and did not occur frequently during our study, making trends difficult to identify. However, the dearth of ratios below 1 indicates that the wake has decayed significantly at such great distances (15D +).

Additionally, the explanation of the scatter of data in Figure 6 is not clear from the data plotted. To some extent, instrumental error may be the culprit behind the variation. Atmospheric conditions potentially contributing to wake strength at these distances are not displayed, but could be explanations for these results.

The data presented in Figure 7 elaborates on the wake decay trend observed in Figure 6. The wake impacts from the centerline of each wake were approximated and plotted against the distances they each represent. Here a clear logarithmic trend is visible, particularly within distances less than 20D from the upwind turbine. After 20D, wind speed ratios between .9 and 1.1 occur. It is unclear if the wakes have impact at this distance or have mostly dissipated by this point. This is especially unclear with the points taken from the interactions between the A- and B-line turbines. Despite this ambiguity, these results are comparable to the Lebrón et al (2009) results on logarithmic wake decay.

The results of wake analysis over long ranges within the wind farm again indicate that the wake dissipates more quickly than in other studies of large offshore wind farms, which require up to twice the downwind distance to achieve the same recovery in wind speed and power output (Barthelmie, 2010).

V. CONCLUSIONS

Wind turbines interacting via the wake generated by the rotating blades greatly impacts the power output at a wind farm. These results confirm that wakes have the most severe impact on power generation during periods of low wind speed and when the wind direction flows directly from one turbine to the next. They are also consistent with previous studies that show that wakes are strongest while close to the point of generation, and then decay logarithmically with distance from that turbine. It appears that for these land-based turbines, wake effects may dissipate over less distance (15-20 D) than for offshore lines of turbines.

Numerical analysis demonstrates strong relationships between atmospheric conditions and the strength of the wakes observed. Wake impacts in the near-turbine region were primarily related to horizontal wind speed. Over greater distances, the relationships between wake impacts and atmospheric conditions vary to include strong ties to temperature, net radiation, and turbulence. More analysis is needed to determine a model reflecting the precise relationship between these, or other potential conditions, and wake impacts.

Observations taken from longer lines of turbines within this same wind farm would be useful as comparison and supplement to this study. It would be interesting to see how the results at the turbines in this study, situated at the periphery of the wind farm, might vary from those central to the farm. Incorporation of LIDAR data as a better indicator of free stream conditions would also be useful, though resource intensive. Wind tunnel experiments would be useful to add control conditions to the multiple variables analyzed in this study.

As wind farms continue to grow, it is increasingly necessary to be able to predict the effects of interacting wakes in an effective and efficient manner. Continuing research in turbine wakes is critical to achieving a levelized cost of wind energy, and thus to industry success.

VI. ACKNOWLEDGMENTS

Support for this research was provided by the U.S. Department of Energy Science Undergraduate Laboratory Internship (SULI) Program under its contract with Iowa State University, Contract No. DE-AC02-07CH11358. Mallory Elise Flowers is grateful to the DOE for the assistantship and opportunity to participate in the SULI program.

Daniel A. Rajewski and Kristopher Spoth preformed data management from the CWEX 2010 and 2011 archives. Russel K. Doorenbos provided the wake projections (as in Figure 2) used for this study.

VII. APPENDICES

A. MATLAB function to variable weights for retrieve normalized wind speed ratio

This program provides the weights, or relative importance, of each variable in relation to the wind speed deficit. To do so, it assumes linear relationships between the observed variables fed and the observed wind speed deficits fed. It treats these as matrices, and solves the equation $\mathbf{A} \times \mathbf{x} = \mathbf{b}$ for x, where **A** is the matrix of observed data with a column for each variable considered, and **b** is a vertical vector of the observed ratios corresponding to the conditions in **A**. Thus, x serves as a coefficient matrix, giving a list of dimensionless coefficients assigned to each variable given. This process will work for matrices of any dimension. For over- or underdetermined systems (more or less sets of data than variables), it calculates the combination of coefficients that yields the least squares solution to the problem. Thus, there will be error in these instances, but it will be minimized for every case (in these results, the average error varied from .25 to .5% for each case). The set of coefficients could be used in predicting normalized wind speed deficits. However, because we know there to be error, and because it is unlikely that there is a perfectly linear formula for normalized wind speed ratios, the program output gives the relative weight for the i^{th} variable: $\text{Weight}_i = \mathbf{x}_i \times \text{median}(\mathbf{A}_i)/\ \text{median}(\mathbf{b}) \times 100\%$.

These weights give us a better view of how important each variable is in computing the normalized wind speed ratio under the given circumstances. Positive values indicate increasing relationship between the corresponding variable and the ratio, whereas negative values indicate a decreasing relationship. Likewise, large absolute values indicate a strong relationship, whereas small absolute values indicate a weak relationship.

The MATLAB script generated to compute the values in this experiment is provided below for additional clarity. Options for both 5- and 6-turbine lines are included. This code is easily adaptable to larger lines of turbines or to different input variables.

```
A = xlsread('SVD analysis.xlsx','2010-B Data','A4:G179');   % Read Data
% b = xlsread('SVD analysis.xlsx','2010-B Data','H4:K179');
b = xlsread('SVD analysis.xlsx','2010-B Data','H4:L179');
[n,m] = size(b);
%% Compute Least Squares Solution for linear coefficients
x = [];
for j=1:n
   [U,S,V] = svd(A);
   Temp = U'*b(j);
```

```
    C = Temp(1:7,1);
    Temp = zeros(7,7);
    for i = 1:7
        Temp(i,i) = (1/S(i,i));
    end
    x = [x,V*Temp*C];
end
%% Return all coefficients as single matrix
% x = [x1,x2,x3,x4];
x = [x1,x2,x3,x4,x5];
%% Compute error: residual as a percent of ws:
err = abs((b-A*x)./b);
% mean_res = [0,0,0,0];
mean_res = [0,0,0,0,0];
% std_res = [0,0,0,0];
std_res = [0,0,0,0,0];
% for i = 1:4
for i = 1:5
    mean_res(i) = sum(err(i,:))/max(size(err));
    std_res(i) = std(err(i,:));
end
mean_res
std_res
%% Read median data for variable weight computation
med_data= xlsread('SVD analysis.xlsx','2010-B Data','A2:G2');
med_a = xlsread('SVD analysis.xlsx','2010-B Data','H2');
med_b = xlsread('SVD analysis.xlsx','2010-B Data','I2');
med_c = xlsread('SVD analysis.xlsx','2010-B Data','J2');
med_d = xlsread('SVD analysis.xlsx','2010-B Data','K2');
med_e = xlsread('SVD analysis.xlsx','2010-B Data','L2');
% med_ratios = [med_a,med_b,med_c,med_d];
med_ratios = [med_a,med_b,med_c,med_d,med_e];
%% Convert coefficients to variable weights
temp = zeros(size(x));
for i = 1:7
    for j=1:5
        temp(i,j) = x(i,j).*med_data(i);
    end
end
% for i = 1:4
for i = 1:5
    for j=1:7
        temp(j,i) = temp(j,i)/med_ratios(i);
    end
end
w = temp
```

B. Additional graphs of interest

Time (Year)	A-line (East Wind)	B-line (East Wind)	B-line (West Wind)
2010	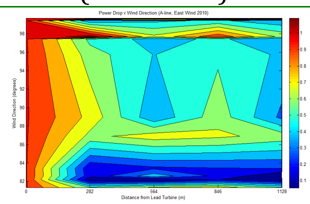	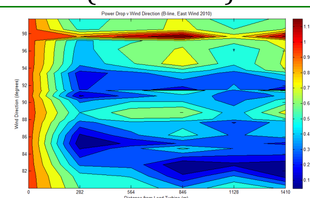	
2011	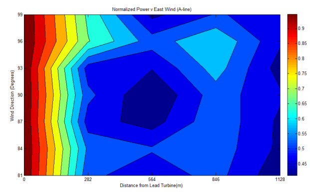	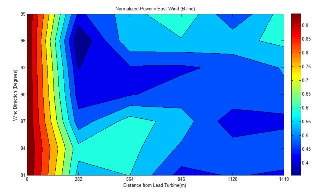	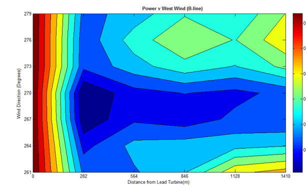

Figure 8: *Power generated compared to wind direction for 2010 and 2011. Visual comparison confirms that power loss due to wake effects is most severe as wind blows straight down the line of turbines. Horizontal wind speed, net radiation, and stability were other conditions for which trends could be approximated through visual comparison in this fashion. Similar samples from other variables do not reveal trends this clearly.*

Time (Diurnal, Year)	A-line (East Wind)	B-line (East Wind)	B-line (West Wind)
2010	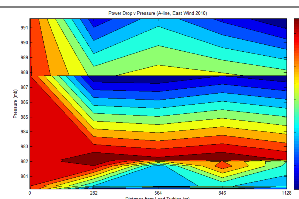	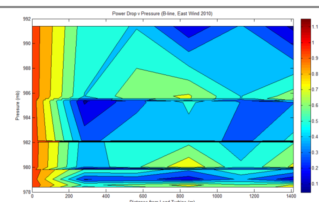	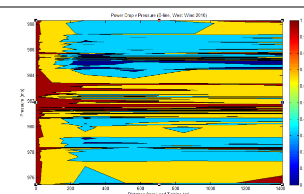
Day, 2011	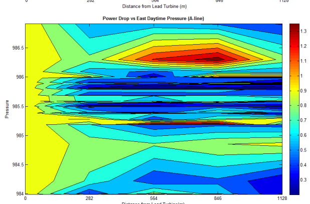	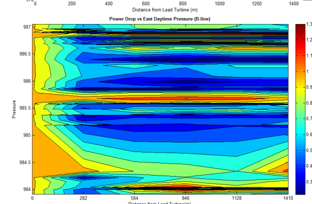	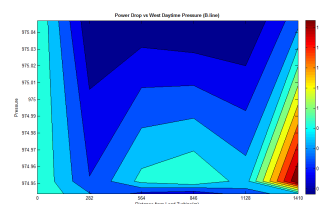
Evening, 2011	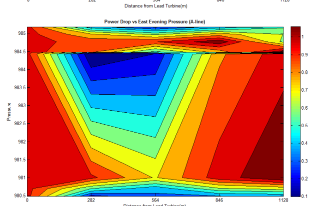	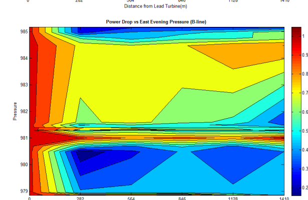	
Morning, 2011	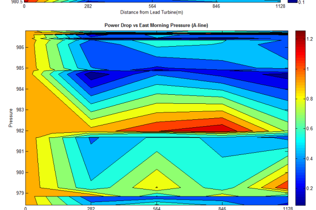	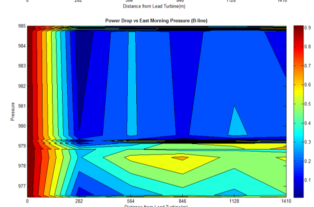	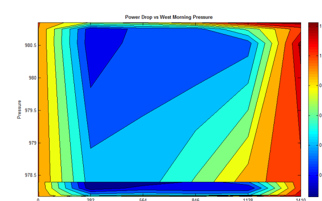

Night, 2011

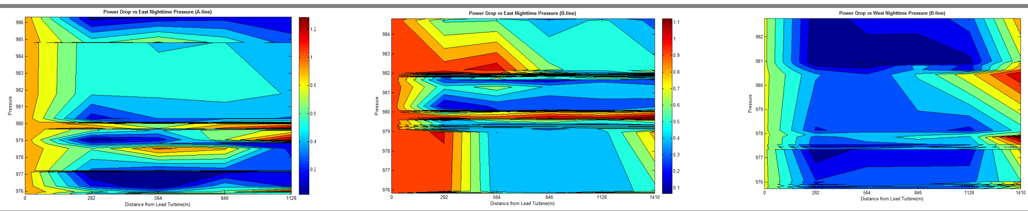

Figure 9: *Power generated compared to surface-level pressure measurements for 2010 and 2011. Visual comparison does not confirm any trends relating power to pressure. Numerical techniques must be employed to isolate pressure changes from other variable conditions. Turbulence data had similar results, meaning trends could not be visually approximated for these conditions. Other conditions analyzed in this fashion revealed clearer trends.*

REFERENCES

Barthelmie, R.J. and Jensen, L.E. 2010: Evaluation of power losses due to wind turbine wakes at the Nysted offshore wind farm, *Wind Energy*, **13**, 573–586, DOI: 10.1002/we.408.

Barthelmie, R.J., Hansen, K., Frandsen, S.T., Rathmann, O., Schepers, J.G., Schlez, W., Philips, J., Rados, K., Zervos, A., Politis, E.S. and Chaviaropoulos, P.K. 2009: Modelling and measuring flow and wind turbine wakes in large wind farms offshore, *Wind Energy*, **12(5)**, 431–444. DOI: 10.1002/we.348.

Barthelmie, R.J., Frandsen, S.T., Nielsen, N.M., Pryor, S.C., Rethore, P.E. and H.E. Jørgensen, 2007: Modelling and measurements of power losses and turbulence intensity in wind turbine wakes at Middelgrunden offshore wind farm, *Wind Energy* doi: 10.1002/we.238. **10**, 217-228

Duckworth, A. and Barthelmie, R.J. 2008: Investigation and validation of wind turbine wake models. *Wind Engineering*, **32(5)**, 459-475.

Hegberg, Turbine Interaction in Large Offshore wind farms, *Atmospheric boundary layer above a wind farm*. August 2004

Barthelmie, R. J., G. C. Larsen, S. T. Frandsen, L. Folkerts, K. Rados, S. C. Pryor, B. Lange, G. Schepers, 2006: Comparison of Wake Model Simulations with Offshore Wind Turbine Wake Profiles Measured by Sodar. *J. Atmos. Oceanic Technol.*, **23**, 888–901.
doi: http://dx.doi.org/10.1175/JTECH1886.1
Lebron, J., Cal, R.B., Kang, H.,Castillo, S., Meneveau, C., 2009: Interaction Between a Wind Turbine Array and a Turbulent Boundary Layer. *11th Americas Conference on Wind Engineering*.